ChemPubSoc Europe

DOI: 10.1002/batt.201900043

BATTERIES & SUPERCAPS
Articles

Mechanism of Lithium Cation Hopping between Tetragonal Thiophene Cages

Pouya Partovi-Azar*[a] and Daniel Sebastiani[a]

We report on the atomistic mechanism of elementary hopping processes of Li^+ ions in liquid thiophene obtained from ab-initio molecular dynamics simulations. We observe the formation of cage structures which solvate the cation. Besides the actual molecular solvation structure, we provide an analysis of the pathway and timescale of basic Li^+ diffusion steps in terms of coordination by sulfur atoms. We compare our results to the situation in a thiophene derivative, namely 3,4-ethylenedioxythiophene (EDOT). The calculations reveal that in both thiophene and EDOT liquids, a tetrahedral structure is formed around the Li^+ ion. While in the case of the former, the Li cation is coordinated by four sulfur atoms, in the latter case it is surrounded by four oxygens. The tetrahedrons act as cages, which accommodate the cation for a considerable duration (of the order of 100 ps). The elementary diffusion step occurs through a "permeable edge" of the tetrahedron formed by two sulfur (or oxygen) atoms at a characteristic distance. This finding indicates that Li^+ conduction in thiophene derivatives can be improved by rationally designing the compound in such a way that maximizes the occurrence of sulfur atoms at that particular distance from each other.

1. Introduction

Understanding interactions between ions and their surrounding environment, for example solvent molecules, membranes, proteins etc., is of fundamental importance. A first step towards obtaining such a knowledge is to reveal the local structure in the vicinity of an ion. Knowledge on the local structure around an ion not only sheds light on the fundamental interactions between the ions and the encompassing medium, but it also provides valuable details on dynamics of the ions, such as their possible diffusion mechanisms. Therefore, such investigations have far-reaching applications, for example in environmental chemistry, drug design, and energy materials.[1–11]

In particular, lithium-based energy-storage systems have recently attracted much attention due to their high energy densities and relatively cheap production costs.[8–11] The field has also witnessed great strides towards more efficient Li-sulfur batteries, thanks to numerous theoretical and experimental studies aimed at enhancing their cycling performance.[12–17] It has been shown that thiophene-based materials can substantially improve the cyclability of the Li–S batteries by suppressing the diffusion of polar Li-polysulfide molecules back to the electrolyte.[18–21] An atomistic picture on the local structural properties of thiophene-based structures around a Li cation can result in a better understanding of the fundamental processes during lithium diffusion in these systems, which in turn, can lead to design of novel electrolyte compositions and/or protective structures based on thiophene. Theoretical simulations have already provided invaluable insights on diffusion mechanism of Li cations in various environments.[22–27] However, due to possible change in the charge distribution in the vicinity of a solvated ion, the classical simulations may fall short of correct description of interactions at an atomistic level. Therefore, to study such systems, a quantum-mechanical treatment is called for.

In this article, we use quantum-mechanical calculations to accurately investigate the most fundamental processes which dictate the local molecular structure around a solvated Li^+ ion as well as its diffusion in thiophene-based molecular liquids. To this end, we perform extensive density functional theory (DFT)-based ab-initio molecular dynamics (AIMD) simulations to have a better picture of possible dynamical configurations of the first Li cation solvation shell in both thiophene and EDOT liquids. Our dynamics simulations suggest a tetrahedral cage structure of the molecules around the cation while showing a cage-hopping mechanism for the Li^+ in thiophene liquid.

Computational Methods

We simulate the dynamics of a single lithium cation in thiophene and EDOT liquids by considering a typical Li^+ concentration of about 1 M. This roughly corresponds to one Li cation in a $12\times12\times12$ Å^3 simulation box. To have an assessment on possible finite-size effects, we additionally consider a larger cell of $20\times20\times20$ Å^3 for thiophene liquid. According to liquid thiophene and EDOT mass densities, namely 1.051 gr/cm^3 and 1.331 gr/cm^3, respectively, the smaller unit cells consist of 13 thiophenes and 10 EDOTs, while the larger simulation cell for thiophene consist of 60 molecules. This results in 117 and 540 atoms altogether in thiophene liquid in the small and large unit cells, respectively. The total number of atoms in the EDOT system is 150.

First, we equilibrate ten samples of pure thiophene and EDOT liquids at 300 K for 5 ns using GROMOS11 (54A7) force field[28] as implemented in GROMACS.[29,30] Afterwards, the ten final structures are extracted from the classical trajectories for each liquid. Then we

[a] Dr. P. Partovi-Azar, Prof. D. Sebastiani
Institute of Chemistry
Martin-Luther-University Halle-Wittenberg
Von-Danckelmann-Platz 4, 06120 Halle, Germany
E-mail: pouya.partovi-azar@chemie.uni-halle.de

perform a quenching by optimizing the geometry of each structure at DFT level. The lowest-energy structures are then used as starting points for DFT-based AIMD simulations, where each liquid is thermalized at 300 K in the canonical ensemble for additional 30 ps.

The DFT calculations are performed using the mixed Gaussian and plane-wave code CP2K/QUICKSTEP[31] in conjunction with a double-ζ DZVP-MOLOPT Gaussian basis set,[32] Goedecker-Teter-Hutter pseudo potentials,[33,34] and the Perdew-Burke-Ernzerhof (PBE) exchange-correlation functional.[35] To account for long-range dispersion interactions, the semi-empirical DFT-D3 method[36] is used. A real-space grid is represented by a plane-wave energy cutoff of 300 Ry. The force criteria for the geometry optimizations based on BFGS[37,37–40] optimizer is set to 0.02 eV/Å. Finally, the time-step for the AIMD simulations is set to 1 fs.

After initial equilibration of the pure systems, the Li ion is added to the $12\times12\times12$ Å^3 unit cells while setting the total charge per unit cell to $+1$. From these starting configurations a second AIMD simulation is performed at 300 K on each liquid for ~360 ps in the canonical ensemble.

2. Results and Discussion

All results presented in this section correspond to our quantum mechanical simulations. Figure 1 shows the gas-phase optimized structures of a thiophene (a) and an EDOT (b) molecule. Figure 1(c) shows the equilibrated structure of 60 thiophene molecules at 300 K in a $20\times20\times20$ Å^3 simulation box, and

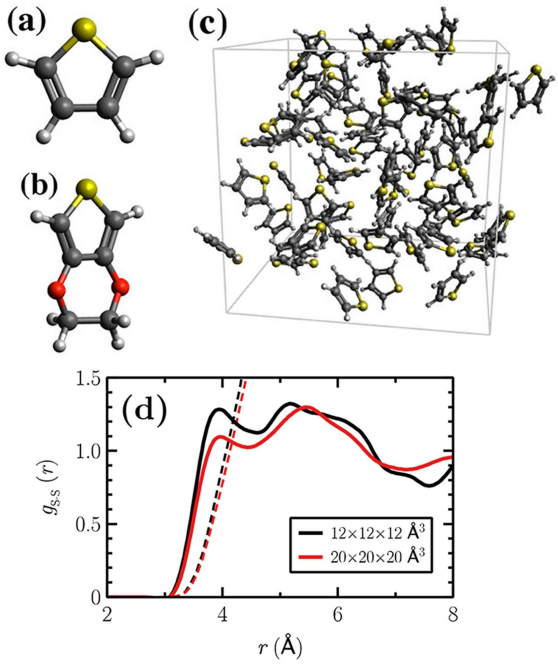

Figure 1. Optimized structures of a) a thiophene and b) an EDOT molecule in vacuum obtained using DFT-based energy minimizations. Hydrogen, carbon, oxygen, and sulfur atoms are shown in white, gray, red, and yellow spheres, respectively. c) Equilibrated structure of 60 thiophene molecules at 300 K in a $20\times20\times20$ Å^3 simulation box. d) shows the S···S radial distribution functions in the pure thiophene liquids in $12\times12\times12$ Å^3 and $20\times20\times20$ Å^3 simulation boxes. Also shown in dashed lines are the coordination numbers

Figure 1(d) shows the sulfur-sulfur radial distribution functions in the pure thiophene liquids in different simulation boxes. Also shown in dashed lines are the corresponding coordination numbers as a functional of sulfur-sulfur distance, r. The results in Figure 1 are obtained from the last 20 ps out of 30 ps AIMD trajectories. As seen in Figure 1(c), despite small differences in dynamical properties of pure thiophene obtained from the unit cells with different sizes, the main features are well captured in the smaller unit cell, that is $12\times12\times12$ Å^3. Therefore, we conclude that the finite-size effects on the local dynamical properties are rather small. Furthermore, as stated earlier, this box is chosen in accordance to typical Li^+ concentration, namely 1 M, in the Li-based batteries. Therefore, in the rest of this section we present the results which correspond to the properties of the thiophene and EDOT liquids in the vicinity of a Li cation in $12\times12\times12$ Å^3 unit cells.

Figure 2(a) shows the displacement of the Li^+ in the thiophene liquid (upper panel) as well as the potential energy of the system (lower panel) as a function of the simulation time. The displacement curve shows two discrete hopping process for the Li cation. The vertical color bars in Figure 2(a) show the time intervals in which the Li^+ is almost stationary (blue) and in a transition state (red). The coordination numbers n_{Li-S} corresponding to these time intervals are shown in Figure 2(b) as functions of the Li···S distance r with the same color coding. As seen in the figure, n_{Li-S} remains almost bound between three and four. In the intervals highlighted by the blue bars in Figure 2(a), the coordination number approaches four, while in the red intervals it becomes closer to three at around 4 Å. Similar results for a Li cation solvated in the EDOT liquid are presented in Figures 2(c) and (d). In contrast to the case of thiophene, no apparent Li^+ hopping is seen in Figure 2 (c), with a small bump in the Li^+ displacement which signals a possible transition in 250–300 ps interval highlighted by a gray vertical bar. However, the displacement of the Li^+ approaches the average value in the 150–200 ps interval. This clearly indicates a sturdier network of solvent molecules which prevents the Li^+ from moving. This is due to stronger interaction between the EDOT molecules which, unlike the thiophene liquid, is brought about by the additional intermolecular hydrogen bonding. The stronger intermolecular interactions in the EDOT liquid also make a local structure similar to the thiophene liquid, where the Li cation is coordinated by four sulfur atoms from the neighboring molecules, unfavorable because of the fact that such a structure would lead to a rather enormous energy penalty due to necessity of an extensive molecular rearrangement. As such, the Li^+ in the EDOT liquid is coordinated by four oxygen atoms from the surrounding molecules. Moreover, in the EDOT liquid, the Li···O nearest-neighbor distance is around 2 Å. In comparison to the Li^+ in thiophene liquid, this results in a stronger electrostatic interaction between the cation and the lone electron pairs of oxygens which further reduces the total energy and, therefore, hinders the Li^+ diffusion.

Analysis of the trajectories indicates formation of tetrahedrons around the Li cation formed by four sulfur and four oxygens in the thiophene and EDOT liquids, respectively.

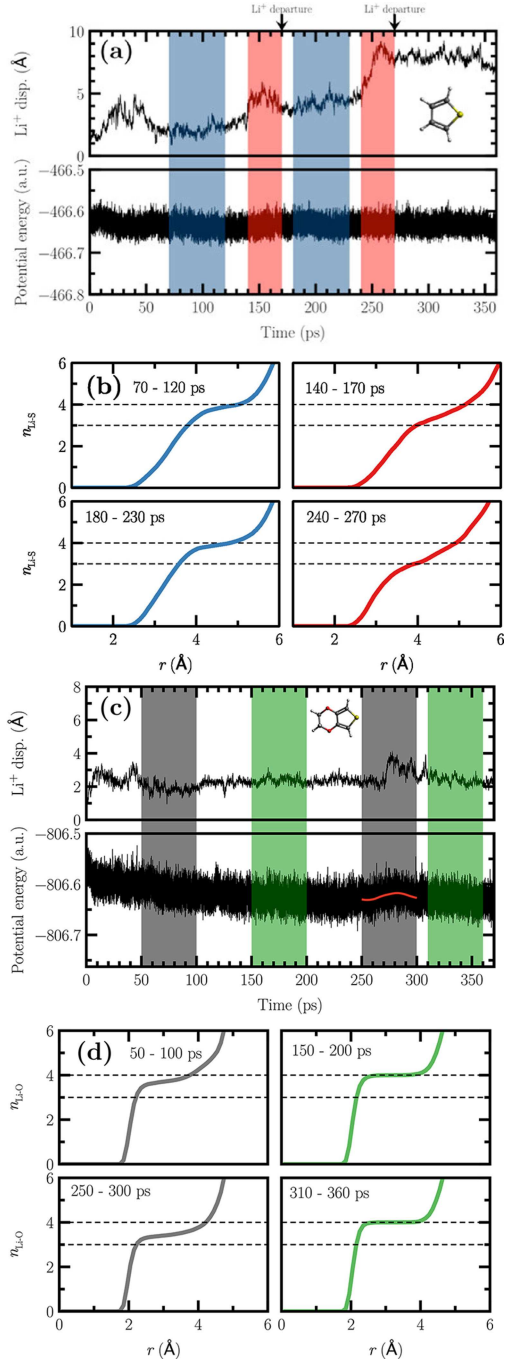

Figure 2. Displacement of the Li^+ in a) thiophene and b) EDOT solvents. Also shown in a) and c) are the corresponding potential energies of the systems during the AIMD simulations. b) and d) show the coordination numbers of the Li cation in thiophene and EDOT liquids, respectively. The colors in b) and d) correspond to the vertical bars in a) and c) with the same colors. The red curve in the lower panel of c) shows a local regression fit to the potential energy from 250 to 300 ps.

Similar tetrahedron structures formed by four oxygen atoms around the Li cation have been previously reported in bulk organic solvents ethylene carbonate, ethyl methyl carbonate, and their mixture.[27] Two typical structures of such tetrahedrons in the thiophene and EDOT liquids obtained from our simulations are shown in Figure 3. The structures are extracted

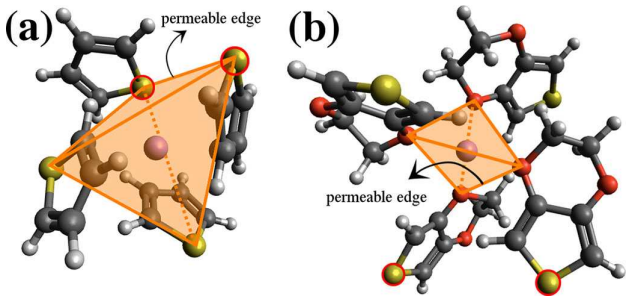

Figure 3. Optimized structures of typical tetrahedrons around the Li cation formed a) by four sulfur atoms and b) by four oxygen atoms in the thiophene and EDOT liquids, respectively. The shown clusters are extracted from the AIMD trajectories and further optimized in vacuum at DFT level.

from stationary parts of the AIMD trajectories, that is the highlighted intervals with blue and green bars in Figures 2(a) and (c), respectively, and further optimized in vacuum using DFT-based energy minimization. The energy per particle of the structure involving an EDOT tetrahedron in Figure 3(b) is about 33% lower than that involving thiophene molecules in (a). Additionally, the volume of the EDOT tetrahedron is approximately 4 times smaller than that of the thiophene. However, all tetrahedral "cages" formed around the Li cation in both liquids are found to share a common structural feature: due to the presence of the cation, two sulfur atoms remain closer to each other compared to other S···S distances in a cage. In a thiophene tetrahedral cage, the shortest S···S distance remains close to 3.95 Å which corresponds to the first peak in the radial distribution functions shown in Figure 1(d). The sulfur atoms forming the shortest S···S distance in a cage are highlighted in Figure 3 with red circles around them. All other S···S distances in a thiophene tetrahedron become 50–100% longer. This results in irregular tetrahedrons around the Li cations, shown in Figure 3 in orange color, with one edge shorter than the others. We observe that the Li^+ always departs from a tetrahedral cage through this edge. Therefore, here we refer to it as a "permeable edge". In the transition configurations, where both n_{Li-S} and n_{Li-O} in Figure 2 reduce from four to three, the cation is observed to be surrounded by two sulfur (oxygen) atoms forming the permeable edge plus an extra sulfur (oxygen) atom belonging to another thiophene (EDOT) molecule from the second solvation shell.

Because we only observe Li^+ cage-hopping in the thiophene liquid, from here on we concentrate on our findings on the atomistic mechanism of Li cation diffusion in the thiophene liquid. We observe that a thiophene tetrahedral cage retains its structure for ~70 ps before the Li^+ escapes the cage through a permeable edge. This transition phase takes approximately ~30 ps before the cation fully departs from the cage and gets trapped in a newly formed tetrahedron cage. As indicated by arrows in Figure 2(a), in the course of our 360 ps AIMD trajectories, we observe two Li^+ departures occurring at $t = 170$ ps and $t = 270$ ps. The Li cation departures are found to be rather fast in both events and take less than 10 ps. Here, we refer to the mechanism for Li^+ diffusion as "cage hopping". This mechanism is shown in Figure 4. The overall process

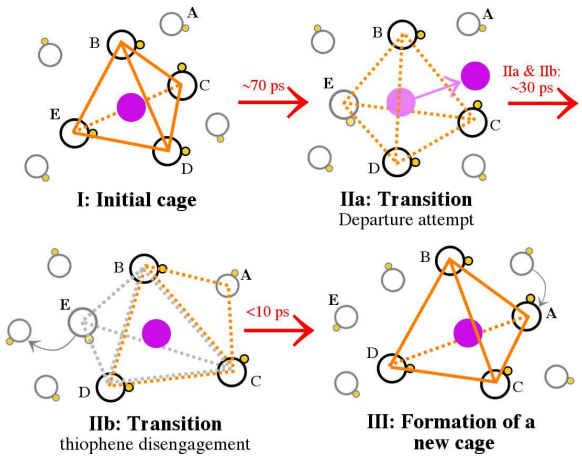

Figure 4. Cage-hopping mechanism of Li^+ diffusion in liquid thiophene revealed by our AIMD simulations. Thiophene molecules are denoted by black and gray colors in the first and second Li cation solvation shells, respectively. The thiophene molecule in the second solvation shell which gets extracted from (attached to) the tetrahedral structures during a Li^+ hop is denoted by E (A). The other thiophene molecules which participate in the structures of both tetrahedrons are labeled as B, C, and D. The Li^+ is shown in purple. Processes shown in steps IIa and IIb for the transition structures occur rather simultaneously and take about 30 ps, while the tetrahedral cage structures retain their configurations for ~70 ps. The permeable edges during the two cage-hopping processes are BC and AB, respectively.

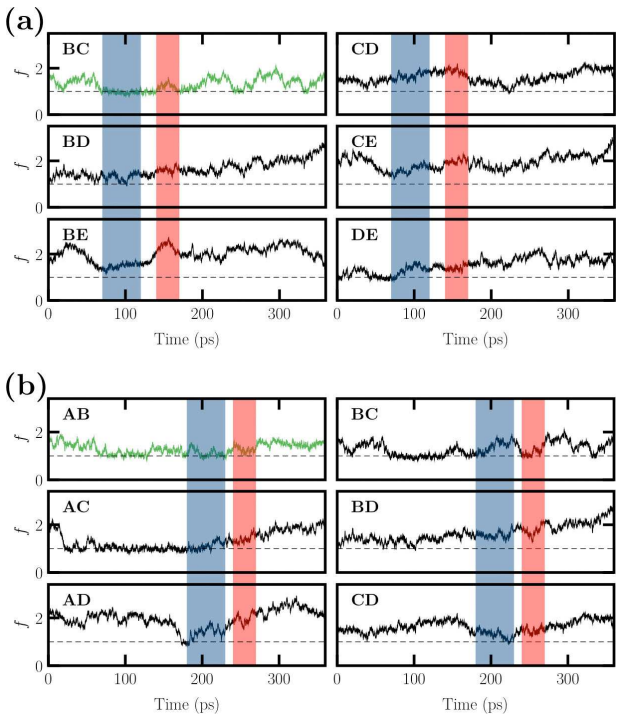

Figure 5. The dimensionless function f during a) the first and b) the second observed Li^+ cage-hoppings in the thiophene liquid. The labels in each panel corresponds to the thiophene molecules in Figure 4. Blue (red) vertical bars are the same as the ones shown in Figure 2(a).

observed during a transition phase is as follows: as the Li cation leaves the cage (illustrated separately as step IIa in Figure 4 for clarity), the farthest thiophene molecule to the permeable edge (denoted as E) disengages from the cage structure (step IIb), while the remaining three eventually form a new tetrahedral cage around the cation together with another thiophene molecule from the second solvation shell (denoted as A in Figure 4). Although the two processes IIa and IIb in Figure 4 are shown in two separate steps for more clarity, but we observe that they occur simultaneously. In order to acquire an atomistic picture on the evolution of the tetrahedral structures upon Li^+ departure, we define dimensionless a function, f, as

$$f = d_{S-S}/d_{S-S}^{nn,l},$$

where d_{S-S} denote the six S···S distances on a tetrahedron and $d_{S-S}^{nn,l} = 3.95$ Å is the nearest neighbor S···S distance in pure thiophene liquid (please see Figure 1(c)). Figure 5 shows the function f during the observed two Li^+ hops in the thiophene liquid in (a) 70–170 and (b) 180–270 ps intervals. The colored bars are similar to those shown in Figure 2(a). Additionally, the labels in each panel correspond to the thiophene molecules in Figure 4. The permeable edge in the first Li^+ hopping event is BC, while in the second one it is denoted as AB. The function f for the S···S distances BC and AB are shown in Figure 5 in green color. These are the only two S···S distances for which f remains around 1 during the interval where their respective tetrahedron structure is stable (shown in blue bars). All other five relative S···S distances undergo a 50–100% increase in the same time intervals. During the intervals highlighted by red bars, however, the f functions for both BC and AB increase. The above observations bring us to the following conclusion: in a thiophene tetrahedral cage, the Li cation is mostly attracted towards the sulfur pair with the S···S distance comparable to the favorable S···S distance in pure thiophene liquid. This is likely a direct consequence of the electrostatic interaction of the cation with the lone electron pairs of the sulfur atoms. Additionally, the eventual escape of the Li^+ is seemingly further facilitated by the thiophene molecules in the second Li cation solvation shell. The relative distances of the sulfur atoms in the B and C thiophenes with that in the A from the second Li^+ solvation shell, namely AB and AC shown in Figure 5(b), also assume values close to 1 during the first Li cation hop, that is 70–170 ps. This means that the presence of the thiophene A with the favorable S···S distance from B and C assists the Li^+ escape through the BC permeable edge possibly due to further enhancement of the electrostatic attraction. As shown in Figure 4, the thiophene A together with B, C, and D form a new tetrahedral cage around the Li cation. As such, we are able to reveal the atomistic mechanism of the Li^+ diffusion in thiophene liquid. In analogy to protonation dynamics in liquid water, the transient S···Li^+···S structures can be identified as the equivalent of a Zundel cation (H_2O···H^+···OH_2). From a rational design perspective, the fact that the diffusion always occurs through the permeable edge where the S···S distance is about 4 Å suggests that in order to have a good Li^+ conductive material based on thiophene, the molecular structure should be designed such as to maximize the occurrence of this particular distance between sulfur atoms. It is worth noting that this distance is shorter than the typical dimensions of Li-polysulfide forming at the early discharge stages of Li–S

batteries.[41] Additionally, it has been shown that the Li-polysulfides tend to form clusters due to their polar nature.[15] The resulting cluster structures usually emerge with typical dimensions which are also longer than the above S···S distance, even for the case of smaller Li-polysulfides. Therefore, a material designed with the above structural feature would not only be a good Li^+ conductor but would also hinder the Li-polysulfide shuttle effect at the same time. Additionally, the proposed structure function, f, can be used as a proper collective variable in meta-dynamics simulations on similar systems and/or as a criterion for the estimation of cage-breaking probability, for example, in kinetic Monte-Carlo simulations on much larger systems.

Similar mechanism is observed in the case of EDOT liquid. However, despite of the fact that the EDOT cage opening process does occur, but the Li cation is observed to be pulled back to the center of the EDOT tetrahedron before being able to form a new cage with additional EDOT molecules in the second solvation shell. This process results in a variation in the potential energy curve shown in Figure 2(c) at 250–300 ps interval of about 272 meV. Such a change in the potential energy is hard to see in the case of Li^+ in thiophene liquid (please see Figure 2(a)). This is possibly due to more flexibility of the thiophene molecules in the liquid compared to the EDOT which blurs such small potential energy changes. To have an estimation on the energy barrier for the cage opening process in the thiophene liquid, we use Eyring-Polanyi equation,[42] where the Gibbs free energy of activation is given by $\Delta G = RT\ \ln(\kappa\ k_b T/h\ r)$. Here, R, k_b, and h are ideal gas, Boltzmann, and Planck's constants, respectively. r is the reaction rate and T is the absolute temperature. We assume that the transmission coefficient, κ, is equal to one. Excluding the first 50 ps of the simulation time, here we consider two cage-opening processes in the case of thiophene. As such, the Gibbs free energy of activation is calculated to be 177 meV in thiophene liquid.

3. Conclusions

Using extensive ab-initio molecular dynamics simulations, we have explored the dynamical structure of thiophene and thiophene-based molecules in the first solvation shell of Li^+ at typical experimental cation concentration. We have shown that the thiophene and EDOT molecules form a tetrahedral cage around the Li cation. In the thiophene cage, the Li^+ is coordinated by four sulfur atoms while in the case of EDOT, it is surrounded by four oxygen atoms. In both tetrahedral cages, we observe one S···S pair at a somewhat shorter distance compared to other S···S distances on a cage which forms a permeable edge. In the case of thiophene, the cage retains its structure for ~70 ps before the Li^+ exits the cage through the tetrahedron's permeable edge. The permeable edge in the thiophene tetrahedral cage is formed by two sulfur atoms at a distance comparable to the nearest-neighbor distance in pure thiophene liquid, namely ~4 Å. All other S···S distances in the tetrahedral cage are 50–100% longer than this value. The Li^+ departure from a thiophene tetrahedron is accompanied by formation of a transition structure where the coordination number of the Li^+ reduces from four to three. The transition process takes about 30 ps before the Li cation forms a new tetrahedral cage with an additional thiophene molecule from the second solvation shell. This diffusion mechanism is referred to as "cage hopping". Additionally, the cage opening is seemingly a consequence of enhanced attractive electrostatic interaction between the Li cation and the sulfur atoms forming a permeable edge and bearing a negative effective charge. We have observed that the thiophene molecules from the second Li cation solvation shell also play a role in the cage opening by orienting their sulfur atoms towards the permeable page and, therefore, further enhancing the attractive interaction with the cation.

In the case of the EDOT liquid, only a partial cage opening has been observed in our simulations. However, in order for the Li^+ to completely transfer to a new EDOT cage, it has to overcome an energy barrier which has been found to be higher than a similar one in the thiophene liquid. This is a result of stronger attractive interaction between the Li^+ and four neighboring oxygens in the EDOT tetrahedral cage, as well as more powerful intermolecular interactions due to formation of additional hydrogen bonds. Therefore, we have not observed a complete transfer of the Li cation to a new tetrahedral EDOT cage in our simulations. Based on these observations, we conclude that the Li^+ diffusion in thiophene and thiophene-based liquids is, in general, slow.

From technical point-of-view, our simulations have direct applications in the field of Li-based energy-storage devices, where thiophene-based materials are widely used in cathode protectors, and as separator membranes to prevent the Li-polysulfides from diffusing back to the electrolyte. Our findings suggest that in order to have a good Li^+ conductive material based on thiophene, the molecular structure should be designed such as to maximize the occurrence of particular S···S distance of ~4 Å. This particular distance is, for example, shorter than the typical dimensions of Li-polysulfide forming at the early discharge stages of Li–S batteries. Additionally, Li-polysulfides clusters emerging during the discharge cycles typically have dimensions which are also longer than the above S···S distance. Therefore, a material designed with the above structural feature would not only be a decent Li^+ conductor but would also mitigate the Li-polysulfide shuttle effect. From theoretical view point, our findings on the local structures of the liquids with solvated Li cation, the proposed function f, and the estimated reaction barriers, can be further used to provide an approximation for Li^+ transfer probability from one cage to the other in larger-scale simulations of Li^+ diffusion in thiophene-based systems using, for example, kinetic Monte-Carlo technique. Additionally, the presented findings can be directly used for defining proper collective variables for meta-dynamics simulations on such complex systems.

Acknowledgements

The authors would like to thank the Center for Information Services and High-Performance Computing at the University of Dresden via proposal "Oligothiophenes on nano-structured gold surfaces" (p_oligothiophenes). The authors also gratefully acknowledge DFG funding via SFB/TRR 102 and PA 3141/3-1.

Conflict of Interest

The authors declare no conflict of interest.

Keywords: density functional theory · energy storage · lithium diffusion · molecular dynamics · thiophene

[1] H. Lammert, A. Wang, U. Mohanty, J. N. Onuchic, *J. Phys. Chem. B* **2018**, *122*, 11218–11227.
[2] M. Jardat, V. Dahirel, F. Carnal, *J. Mol. Liq.* **2017**, *228*, 224–229.
[3] R. Börner, D. Kowerko, H. G. Miserachs, M. F. Schaffer, R. K. Sigel, *Coord. Chem. Rev.* **2016**, *327*, 123–142.
[4] L.-Z. Sun, D. Zhang, S.-J. Chen, *Annu. Rev. Biophys.* **2017**, *46*, 227–246.
[5] D. E. Draper, D. Grilley, A. M. Soto, *Annu. Rev. Biophys. Biomol. Struct.* **2005**, *34*, 221–243.
[6] S. Mogurampelly, O. Borodin, V. Ganesan, *Annu. Rev. Chem. Biomol. Eng.* **2016**, *7*, 349–371.
[7] Z. Yang, L. Gu, Y.-S. Hu, H. Li, *Annu. Rev. Mater. Res.* **2017**, *47*, 175–198.
[8] M. Park, X. Zhang, M. Chung, G. B. Less, A. M. Sastry, *J. Power Sources* **2010**, *195*, 7904–7929.
[9] V. Etacheri, R. Marom, R. Elazari, G. Salitra, D. Aurbach, *Energy Environ. Sci.* **2011**, *4*, 3243–3262.
[10] M. Wild, L. O'neill, T. Zhang, R. Purkayastha, G. Minton, M. Marinescu, G. Offer, *Energy Environ. Sci.* **2015**, *8*, 3477–3494.
[11] A. Manthiram, Y. Fu, S.-H. Chung, C. Zu, Y.-S. Su, *Chem. Rev.* **2014**, *114*, 11751–11787.
[12] Y.-X. Yin, S. Xin, Y.-G. Guo, L.-J. Wan, *Angew. Chem. Int. Ed. Engl.* **2013**, *52*, 13186–13200.
[13] A. Rosenman, E. Markevich, G. Salitra, D. Aurbach, A. Garsuch, F. F. Chesneau, *Adv. Energy Mater.* **2015**, *5*, 1500212.
[14] Q. Pang, X. Liang, C. Y. Kwok, L. F. Nazar, *Nat. Energy* **2016**, *1*, 16132.
[15] P. Partovi-Azar, T. D. Kühne, P. Kaghazchi, *Phys. Chem. Chem. Phys.* **2015**, *17*, 22009–22014.
[16] P. Partovi-Azar, S. P. Jand, P. Kaghazchi, *Phys. Rev. Appl.* **2018**, *9*, 014012.
[17] A. Hoefling, D. T. Nguyen, P. Partovi-Azar, D. Sebastiani, P. Theato, S.-W. Song, Y. J. Lee, *Chem. Mater.* **2018**, *30*, 2915–2923.
[18] F. Wu, J. Chen, R. Chen, S. Wu, L. Li, S. Chen, T. Zhao, *J. Phys. Chem. C* **2011**, *115*, 6057–6063.
[19] Y. Yang, G. Yu, J. J. Cha, H. Wu, M. Vosgueritchian, Y. Yao, Z. Bao, Y. Cui, *ACS Nano* **2011**, *5*, 9187–9193.
[20] L. Yan, X. Gao, J. P. Thomas, J. Ngai, H. Altounian, K. T. Leung, Y. Meng, Y. Li, *Sustainable Energy Fuels* **2018**, 2, 1574–1581.
[21] J. H. Lee, J. Kang, S.-W. Kim, W. Halim, M. W. Frey, Y. L. Joo, *ACS Omega* **2018**, *3*, 16465–16471.
[22] V. Meunier, J. Kephart, C. Roland, J. Bernholc, *Phys. Rev. Lett.* **2002**, *88*, 075506.
[23] W. Li, S. H. Garofalini, *Solid State Ionics* **2004**, *166*, 365–373.
[24] J. Yang, J. S. Tse, *J. Phys. Chem. A* **2011**, *115*, 13045–13049.
[25] B. Song, J. Yang, J. Zhao, H. Fang, *Energy Environ. Sci.* **2011**, *4*, 1379–1384.
[26] A. Deshpande, L. Kariyawasam, P. Dutta, S. Banerjee, *J. Phys. Chem. C* **2013**, *117*, 25343–25351.
[27] M. T. Ong, O. Verners, E. W. Draeger, A. C. Van Duin, V. Lordi, J. E. Pask, *J. Phys. Chem. B* **2015**, *119*, 1535–1545.
[28] N. Schmid, A. P. Eichenberger, A. Choutko, S. Riniker, M. Winger, A. E. Mark, W. F. van Gunsteren, *Eur. Biophys. J.* **2011**, *40*, 843.
[29] B. Hess, C. Kutzner, D. Van Der Spoel, E. Lindahl, *J. Chem. Theory Comput.* **2008**, *4*, 435–447.
[30] D. Van Der Spoel, E. Lindahl, B. Hess, G. Groenhof, A. E. Mark, H. J. Berendsen, *J. Comput. Chem.* **2005**, *26*, 1701–1718.
[31] J. VandeVondele, M. Krack, F. Mohamed, M. Parrinello, T. Chassaing, J. Hutter, *Comput. Phys. Commun.* **2005**, *167*, 103–128.
[32] J. VandeVondele, J. Hutter, *J. Chem. Phys.* **2007**, *127*, 114105.
[33] S. Goedecker, M. Teter, J. Hutter, *Phys. Rev. B* **1996**, *54*, 1703.
[34] M. Krack, *Theor. Chem. Acc.* **2005**, *114*, 145–152.
[35] J. P. Perdew, K. Burke, M. Ernzerhof, *Phys. Rev. Lett.* **1996**, *77*, 3865.
[36] S. Grimme, J. Antony, S. Ehrlich, H. Krieg, *J. Chem. Phys.* **2010**, *132*, 154104.
[37] C. G. Broyden, *IMA J. Appl. Math.* **1970**, *6*, 76–90.
[38] R. Fletcher, *Comput. J.* **1970**, *13*, 317–322.
[39] D. Goldfarb, *Math. Comput.* **1970**, *24*, 23–26.
[40] D. F. Shanno, *Math. Comput.* **1970**, *24*, 647–656.
[41] L. Wang, T. Zhang, S. Yang, F. Cheng, J. Liang, J. Chen, *J. Energy Chem.* **2013**, *22*, 72–77.
[42] M. G. Evans, M. Polanyi, *Trans. Faraday Soc.* **1935**, *31*, 875–894.

Manuscript received: March 19, 2019
Accepted manuscript online: April 2, 2019
Version of record online: April 25, 2019